Robust Control of an Actuator-Sensor Array for Active Vibration Suppression

Albert Schwinn and Hartmut Janocha
Laboratory for Process Automation (LPA)
Saarland University/Germany

This paper describes a robust active vibration control approach for distributed piezoelectric ceramic patches used as actuators and sensors. A number of symmetrically spaced ceramics have been affixed to a beam where they can perform two different tasks. First, the structural behavior is identified with the help of the ceramics. Second, the grid-array is used for control purposes, the functionality of a patch as an actuator or a sensor being able to change depending on the operating and boundary conditions of the structure. The central focus of the paper is on the applied control approach, which is a robust linear quadratic Gaussian (LQG) control. The uncertainties against which the control approach is robust are parameter uncertainties and spillover.

1 Introduction

Active vibration control plays an increasingly important role in research and industry as more and more lightweight structures are used with the disadvantage of more pronounced vibrations. Induced strain elements, like piezoelectric ceramics as actuators and/or sensors are described in several papers e.g. [4, 7] to be effective for the design of active vibration control. Mainly two approaches have been followed to build the models, namely continuous closed-formulations e.g. [2, 3] and discrete Finite Element Method (FEM) solutions e.g. [6] and often state-feedback control laws have been applied.

In the present paper a different approach is presented. Several ceramic patches are assumed to be bonded onto a structure with a certain, but not exact knowledge of the structural dynamics. The frequency response between every patch is determined in a first step by using one patch as actuator to excite the structure and the others to measure the response.

The same grid array is also used for control purposes, and the functionality of a patch as an actuator or a sensor is defined with an optimization criterion. Each ceramic can serve as an actuator or a sensor or can even combine both functions at the same time [5]. A major advantage of this smart structure concept is that it can rearrange its actuator-sensor configuration on-line if the system characteristics change. In order to

face parameter uncertainties within the model, a robust linear quadratic Gaussian (LQG) control synthesis procedure is applied which is based on a pair of algebraic Riccati equations arising in risk-sensitive optimal control [8]. This leads to a controller which guarantees a certain upper bound on the time-averaged performance of the closed-loop stochastic uncertain system.

2 Experimental setup

The experimental setup consists of an aluminium beam with the dimensions according to Figure 1. It is clamped at both ends and the ceramics

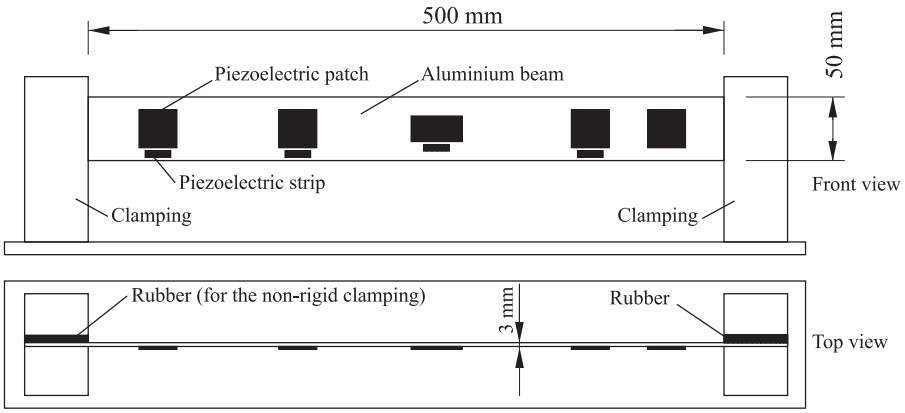

Fig. 1: Clamped beam with bonded piezoelectric ceramics

are glued onto one side. Patches 1-4 can be used for control, and piezo number 5 is used to create a disturbance. The small strips of piezoceramic are intended for the investigation of nearly-collocated actuators and sensors. The ceramic properties are shown in Table 1. Different boundary conditions can be studied with this setup: either rigid clamping without rubber mounts, or soft clamping with the use of a rubber mount.

Ceramic	Size (WxLxT) [mm^3]	Material	Collocated sensor	Size (WxLxT) [mm^3]	Material
$1, 2, 4, 5$	$29.7 \times 29.7 \times 1.0$	PIC 151	$1, 2, 3, 4$	$2.5 \times 20.0 \times 1.0$	PK11
3	$20.0 \times 40.0 \times 1.5$	PIC 151			

Table 1: Dimensions and material of the applied ceramics

3 Identification

In the first step, before the controller can be designed, the patches were used to identify the structural behaviour and to construct a model. In order to perform this experimental modal model identification, a band-limited white noise signal is applied to a selected patch which is used as an actuator and the response is measured at the other patches. With the calculated frequency responses [10] a model of the pole/residue form (1) is established

$$\mathbf{H}_{\mathrm{Model}}(s) = \sum_{\mathrm{j\ identified}} \left(\frac{\mathbf{R}_\mathrm{j}}{s-\lambda_\mathrm{j}} + \frac{\bar{\mathbf{R}}_\mathrm{j}}{s-\bar{\lambda}_\mathrm{j}}\right) + \mathbf{E}. \tag{1}$$

$\mathbf{R}_\mathrm{j}$ and $\bar{\mathbf{R}}_\mathrm{j}$ are the (complex conjugate) residue matrices, λ_j and $\bar{\lambda}_\mathrm{j}$ are the (complex conjugate) poles and $\mathbf{E}$ is a correction matrix in order to account for neglected high-frequency modes. For control purposes one is interested in a state-space model and for this the residues $\mathbf{R}_\mathrm{j}$ were decomposed into a dyad formed of a column vector $\underline{\psi}_\mathrm{jc}$(the modal output) and a row vector $\underline{\psi}_\mathrm{jb}^\mathrm{T}$(the modal input). The following bloc-diagonal state-space model [1] can be calculated as

$$\begin{aligned}
\begin{pmatrix} \dot{\underline{x}}(t) \\ \ddot{\underline{x}}(t) \end{pmatrix} &= \begin{pmatrix} \mathbf{0} & \mathbf{I} \\ -\mathbf{\Omega^2} & -\mathbf{\Gamma} \end{pmatrix} \begin{pmatrix} \underline{x}(t) \\ \dot{\underline{x}}(t) \end{pmatrix} + \begin{pmatrix} \mathbf{0} \\ \mathbf{\Psi}_\mathrm{b}^\mathrm{T} \end{pmatrix} \underline{u}(t) \\
\underline{y}(t) &= \begin{pmatrix} \mathbf{\Psi}_\mathrm{c} & \mathbf{0} \end{pmatrix} \begin{pmatrix} \underline{x}(t) \\ \dot{\underline{x}}(t) \end{pmatrix}.
\end{aligned} \tag{2}$$

$\mathbf{\Omega}^2 = \mathrm{diag}(f_\mathrm{modal}^2)$ is the modal stiffness matrix, formed by the modal frequencies. $\mathbf{\Gamma}$ is the modal damping matrix and $\mathbf{I}$ is the identity matrix. $\mathbf{\Psi}_\mathrm{b}^\mathrm{T}$ is the modal input matrix, formed by the modal input vectors and $\mathbf{\Psi}_\mathrm{c}$ is the modal output matrix, composed of the modal output vectors. $\underline{x}(t)$ is the vector of modal displacements, $\underline{u}(t)$ is the vector of inputs and $\underline{y}(t)$ is the vector of outputs. The state-space model (2) is the basis for the controller design.

4 Selection of actuators and sensors

The ability of an actuator to suppress a mode and that of a sensor to detect a mode depends on its position in relation to the nodes and antinodes of the mode. The residues of the frequency responses between two patches are a measure for the efficiency of this actuator-sensor combination. In order to penalize modes with small residues, which means that this combination cannot actuate or sense a mode, a performance index is calculated as the product of the norm of the residues, normalized by

its maximum value $R_{\mathrm{j,max}}$ over all actuator-sensor combinations. This leads to a performance matrix $\mathbf{P}$ with the elements

$$\begin{aligned} \mathbf{P}(m,p) &= \prod_{\mathrm{j}} \frac{|\mathbf{R}_{\mathrm{j}}(m,p)|}{R_{\mathrm{j,max}}} \quad \begin{array}{lcl} m & : & 1 \ldots n_{\mathrm{Pa}}, \\ p & : & 1 \ldots n_{\mathrm{Pa}}, \\ j & : & 1 \ldots n_{\mathrm{Mo}}. \end{array} \end{aligned} \tag{3}$$

n_{Pa} indicates the total number of ceramics applied to the beam and n_{Mo} indicates the total number of modes which should be considered. The best choice for an actuator-sensor combination is the maximum value of all elements of $\mathbf{P}$: $P_{\mathrm{Best}} = \max(\mathbf{P}(m,p))$. The evaluation of equation (3) for the beam with the boundary conditions 'rigid-clamping' shows that the combination 'actuator 1, sensor 1' has the maximum performance. For the non-collocated case the combination 'actuator 4, sensor 1' is the best choice. This result is obvious for the clamped beam, because the patches 1 and 4 are located near the ends and can sense and actuate all modes in the considered frequency range. Further results can be found in [9]. After the structure is identified and an actuator-sensor configuration is selected, the robust control can be designed.

5 Robust control of uncertain systems

An important class of uncertain system models involves separating the nominal system model from the uncertainty in the system in a feedback interconnection and is shown in Figure 2. The uncertainty Δ is typically a quantity which is unknown but bounded in magnitude. In order

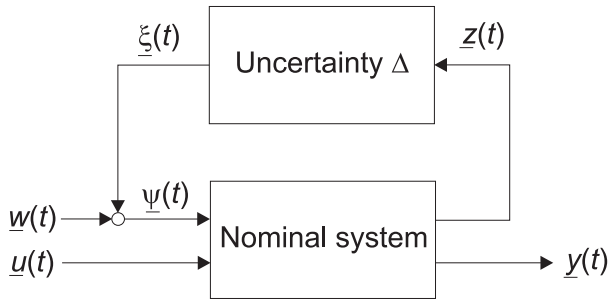

Fig. 2: Uncertain system with noise inputs $w(t)$

to define the minimax LQG control problem, the following stochastic uncertain system is defined in terms of a stochastic state equation

$$\begin{aligned} \mathrm{d}\underline{x}(t) &= (\mathbf{A}\underline{x}(t) + \mathbf{B_1}\underline{u}(t) + \mathbf{B_2}\underline{\xi}(t))\mathrm{d}t + \mathbf{B_2}\underline{w}(t)\mathrm{d}t, \quad x(0) = x_0, \\ z(t) &= \mathbf{C_1}\underline{x}(t) + \mathbf{D_1}\underline{u}(t), \\ \mathrm{d}\underline{y}(t) &= (\mathbf{C_2}\underline{x}(t) + \mathbf{D_2}\underline{\xi}(t))\mathrm{d}t + \mathbf{D_2}\underline{w}(t)\mathrm{d}t, \quad y(0) = 0. \end{aligned} \tag{4}$$

where $\underline{\xi}(\cdot)$ is a stochastic process and $\underline{w}(\cdot)$ is a Wiener process. $u(t)$ is the control input, $y(t)$ is the measured output and the matrices $\mathbf{A}, \mathbf{B_1}, \mathbf{B_2}$, $\mathbf{C_1}, \mathbf{C_2}, \mathbf{D_1}, \mathbf{D_2}$ are matrices of suitable dimensions and depend on the considered uncertainty. The class of admissible uncertain probability measures is defined in [8] and encompasses many important classes of uncertainty arising in control systems e.g. the standard norm-bounded uncertainty constraint, or the H_∞ norm-bounded uncertainty description.

In the minimax optimal control to be considered, attention will be restricted to the following linear output-feedback controller of the form

$$\begin{aligned} \mathrm{d}\underline{x}_\mathrm{c}(t) &= \mathbf{A}_c\underline{x}_\mathrm{c}(t)\mathrm{d}t + \mathbf{B}_c\mathrm{d}\underline{y}(t) \\ \underline{u}(t) &= \mathbf{K}\underline{x}_\mathrm{c}(t). \end{aligned} \tag{5}$$

$\underline{y}(t)$ is the measured input, $\underline{u}(t)$ is the control output and $\underline{x}_\mathrm{c}$ is the state of the controller. For the optimal control the following cost functional $J(\cdot)$ is considered

$$\begin{aligned} J(\underline{u}(\cdot), \underline{\zeta}(\cdot)) &= \limsup_{T\to\infty} \frac{1}{2T}\mathrm{E}^{Q^T}\int_0^T F(\underline{x}(t), \underline{u}(t))\mathrm{d}t, \\ F(x,u) &= \underline{x}'\mathbf{R}\underline{x} + \underline{u}'\mathbf{G}\underline{u}. \end{aligned} \tag{6}$$

E^{Q^T} is the expectation with respect to the probability measure Q^T, corresponding to the set of martingales $\underline{\zeta}$, see [8], and $\mathbf{R}, \mathbf{G}$ are weighting matrices. The minimax optimal control problem is to find a controller of the form (5) which minimizes the worst case value of the cost functional (6) in the face of uncertainty. The solution of the infinite horizon LQG control problem is given by the following two parameter-dependent algebraic Riccati equations

$$\begin{aligned} &(\mathbf{A} - \mathbf{B}_2\mathbf{D}_2'\mathbf{\Gamma}^{-1}\mathbf{C}_2)\mathbf{Y}_\infty + \mathbf{Y}_\infty(\mathbf{A} - \mathbf{B}_2\mathbf{D}_2'\mathbf{\Gamma}^{-1}\mathbf{C}_2)' \\ &-\mathbf{Y}_\infty(\mathbf{C}_2'\mathbf{\Gamma}^{-1}\mathbf{C}_2 - \frac{1}{\tau}\mathbf{R}_\tau)\mathbf{Y}_\infty + \mathbf{B}_2(\mathbf{I} - \mathbf{D}_2'\mathbf{\Gamma}^{-1}\mathbf{D}_2)\mathbf{B}_2' = 0 \end{aligned} \tag{7}$$

$$\begin{aligned} &\mathbf{X}_\infty(\mathbf{A} - \mathbf{B}_1\mathbf{G}_\tau^{-1}\mathbf{\Upsilon}_\tau') + (\mathbf{A} - \mathbf{B}_1\mathbf{G}_\tau^{-1}\mathbf{\Upsilon}_\tau')'\mathbf{X}_\infty \\ &+(\mathbf{R}_\tau - \Upsilon_\tau\mathbf{G}_\tau^{-1}\Upsilon_\tau') - \mathbf{X}_\infty(\mathbf{B}_1\mathbf{G}_\tau^{-1}\mathbf{B}_1' - \frac{1}{\tau}\mathbf{B}_2\mathbf{B}_2')\mathbf{X}_\infty = 0 \end{aligned} \tag{8}$$

with $\mathbf{\Gamma} = \mathbf{D}_2\mathbf{D}_2' > 0$, $\mathbf{R}_\tau = \mathbf{R} + \tau\mathbf{C}_1'\mathbf{C}_1$, $\mathbf{G}_\tau = \mathbf{G} + \tau\mathbf{D}_1'\mathbf{D}_1$ and $\mathbf{\Upsilon}_\tau = \tau\mathbf{C}_1'\mathbf{D}_1$. For the solution of (7) and (8) the following must be fulfilled: The pair $((\mathbf{A}-\mathbf{B}_2\mathbf{D}_2'\mathbf{\Gamma}^{-1}\mathbf{C}_2), (\mathbf{B}_2(\mathbf{I}-\mathbf{D}_2'\mathbf{\Gamma}^{-1}\mathbf{D}_2)))$ is stabilizable and for a constant $\tau > 0$ the matrix $\mathbf{Y}_\infty$ is positive-definite, $\mathbf{X}_\infty$ is nonnegative-definite and $(\mathbf{I} - \frac{1}{\tau}\mathbf{Y}_\infty\mathbf{X}_\infty)$ has only positive eigenvalues. Then the

optimal risk-sensitive controller is a controller of the form (5) with

$$\begin{aligned}
\mathbf{K} &= -\mathbf{G}_\tau^{-1}(\mathbf{B}_1\mathbf{X}_\infty + \mathbf{\Upsilon}_\tau') \\
\mathbf{A}_c &= \mathbf{A} + \mathbf{B}_1\mathbf{K} - \mathbf{B}_c\mathbf{C}_2 + \frac{1}{\tau}(\mathbf{B}_2 - \mathbf{B}_c\mathbf{D}_2)\mathbf{B}_2'\mathbf{X}_\infty \\
\mathbf{B}_c &= (\mathbf{I} - \frac{1}{\tau}\mathbf{Y}_\infty\mathbf{X}_\infty)^{-1}(\mathbf{Y}_\infty\mathbf{C}_2' + \mathbf{B}_2\mathbf{D}_2')\mathbf{\Gamma}^{-1}.
\end{aligned} \tag{9}$$

The constant $\tau > 0$ is chosen, such that $\inf_\tau(V_\tau^0 + \tau d)$ is reached, with

$$\begin{aligned}
&V_\tau^0 = \\
&\tfrac{1}{2}\mathrm{tr}[\mathbf{Y}_\infty\mathbf{R}_\tau + \\
&\quad (\mathbf{Y}_\infty\mathbf{C}_2' + \mathbf{B}_2\mathbf{D}_2')\mathbf{\Gamma}^{-1}(\mathbf{C}_2\mathbf{Y}_\infty + \mathbf{D}_2\mathbf{B}_2')\mathbf{X}_\infty(\mathbf{I} - \tfrac{1}{\tau}\mathbf{Y}_\infty\mathbf{X}_\infty)^{-1}].
\end{aligned} \tag{10}$$

It is shown in [8] that this controller is an absolutely stabilizing controller for the stochastic uncertain system and guarantees an upper bound on the cost functional (6).

6 Application of the robust control synthesis procedure

Two different kinds of uncertainties are considered in the following and the controller design is shown, based on the results of the section above. First, neglected higher frequency-dynamics (NHFD) and then model errors (ME) will be considered. The first uncertainty will be realized by a frequency weighted multiplicative uncertainty as shown in Figure 3.

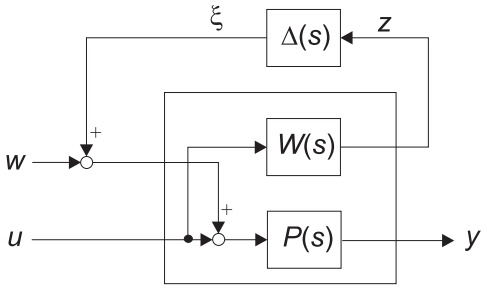

Fig. 3: Uncertain system for neglected higher frequency-dynamics

The true transfer function P_Δ is assumed to be

$$P_\Delta(s) = \frac{y}{u} = P(s)[1 + \Delta(s)W(s)], \tag{11}$$

where $P(s)$ is the nominal transfer function, $W(s)$ is a suitable weighting transfer function and $\Delta(s)$ is an uncertain transfer function satisfying

the H_∞ norm bound. Hence it follows

$$\left| \frac{P_\Delta(\mathrm{j}\omega) - P(\mathrm{j}\omega)}{P(\mathrm{j}\omega)} \right| \leq |W(\mathrm{j}\omega)| \,. \tag{12}$$

Figure 4 shows an example of the realization of (12). The function $W(\mathrm{j}\omega)$ was chosen to consist of a 4th-order Tschebycheff high-pass filter, added to a 4th-order low-pass Bessel-filter, in order to smooth the low-frequency response. One can see in Figure 4 that condition (12) is not fulfilled at all frequencies, but it was found in practice, that this is unnecessary in order to obtain the required level of robustness. The

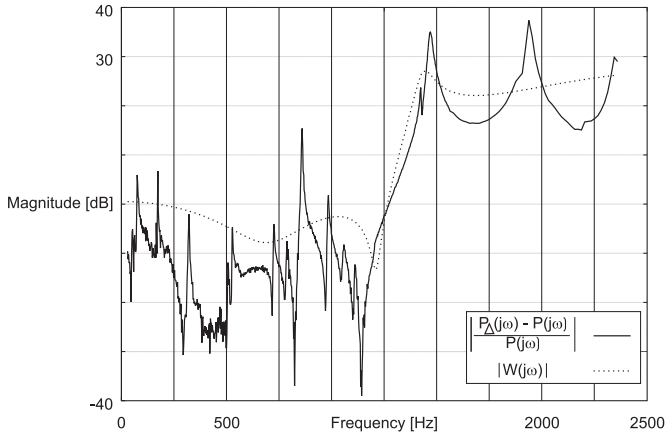

Fig. 4: Multiplicative uncertainty bound

stochastic uncertain system (4) which must be built for the controller design is obtained from a state-space realization of the transfer function $P(s)$ augmented with the transfer function $W(s)$.

The second uncertainty to be considered are model errors. In this respect the following will be assumed. Consider an uncertain element f of the nominal state-space matrices (13)

$$\begin{bmatrix} \underline{\dot{x}} \\ \underline{y} \end{bmatrix} = \begin{bmatrix} \mathbf{A} & \mathbf{B} \\ \mathbf{C} & \mathbf{D} \end{bmatrix} \begin{bmatrix} \underline{x} \\ \underline{u} \end{bmatrix}, \tag{13}$$

with the error model

$$\begin{aligned} f &= f_0(1 + b_0\delta), \quad -1 < \delta < +1 \\ \mathbf{\Delta} &= \delta \mathbf{I}. \end{aligned} \tag{14}$$

Each uncertain element of the matrices $\mathbf{A}, \mathbf{B}, \mathbf{C}$ or $\mathbf{D}$ leads to an additional uncertainty input/output and the system matrix (13) must be

extended as follows. The nominal element will be f_0 and the diagonal will be extended with zero, belonging to one additional uncertainty input/output. The element in the row of the nominal element and the column of the extended input is f_0. The element in the column of the nominal element and the row of the extension is b_0. An example for an uncertain element in the matrix $\mathbf{A}$ is shown in equation (15):

$$\begin{bmatrix} \dot{x}_1 \\ \vdots \\ \dot{x}_\mathrm{j} \\ \vdots \\ \dot{x}_\mathrm{n} \\ z_\mathrm{i} \\ y_1 \\ \vdots \\ y_\mathrm{p} \end{bmatrix} = \begin{bmatrix} a_{11} & \dots & a_{1\mathrm{l}} & \dots & a_{1\mathrm{n}} & 0 & b_{11} & \dots & b_{1\mathrm{q}} \\ \vdots & \ddots & \vdots & \ddots & \vdots & \vdots & \vdots & \ddots & \vdots \\ a_{\mathrm{j}1} & \dots & \mathbf{f}_{0,\mathrm{i}} & \dots & a_{\mathrm{j}\mathrm{n}} & \mathbf{b}_{0,\mathrm{i}} & b_{\mathrm{j}1} & \dots & b_{\mathrm{j}\mathrm{q}} \\ \vdots & \ddots & \vdots & \ddots & \vdots & \vdots & \vdots & \ddots & \vdots \\ a_{\mathrm{n}1} & \dots & a_{\mathrm{n}\mathrm{l}} & \dots & a_{\mathrm{n}\mathrm{n}} & 0 & b_{\mathrm{n}1} & \dots & b_{\mathrm{n}\mathrm{q}} \\ 0 & \dots & \mathbf{f}_{0,\mathrm{i}} & \dots & 0 & \mathbf{0} & 0 & \dots & 0 \\ c_{11} & \dots & c_{1\mathrm{l}} & \dots & c_{1\mathrm{n}} & 0 & d_{11} & \dots & d_{1\mathrm{q}} \\ \vdots & \ddots & \vdots & \ddots & \vdots & \vdots & \vdots & \ddots & \vdots \\ c_{\mathrm{p}1} & \dots & c_{\mathrm{p}\mathrm{l}} & \dots & c_{\mathrm{p}\mathrm{n}} & 0 & d_{\mathrm{p}1} & \dots & d_{\mathrm{p}\mathrm{q}} \end{bmatrix} \begin{bmatrix} x_1 \\ \vdots \\ x_\mathrm{j} \\ \vdots \\ x_\mathrm{n} \\ \xi_\mathrm{i} \\ u_1 \\ \vdots \\ u_\mathrm{q} \end{bmatrix} \tag{15}$$

If we assume that only the modal-frequency and damping in the matrix $\mathbf{A}$ are uncertain, we obtain the following matrices for equation (4)

$$\mathbf{B}_1 := \mathbf{B}, \quad \mathbf{B}_2 := [0 \dots b_{0,\mathrm{i}} \dots 0]', \quad \mathbf{C}_2 := \mathbf{C}, \tag{16}$$

$$\mathbf{C}_1 := [0 \dots f_{0,\mathrm{i}} \dots 0], \quad \mathbf{D}_1 := \mathbf{0}$$

These matrices will be used for the calculation of a robust controller as indicated in section 5, which is robust against parameter uncertainties.

7 Results

In the following some results for the above calculated controllers are presented. Figures 5 and 6 illustrate the active vibration suppression which has been achieved with the robust LQG control. Figure 5 shows the power spectrum of the sensor voltage measured at ceramic 2 for two different actuator/sensor combinations and the application of NHFD uncertainty. The boundary conditions were 'rigid clamping on both ends' and the first six modes were identified for the model. One can see that no spillover occurs, which was the objective of this uncertainty description. The achievable suppression depends heavily on the weighting transfer function and the matrices $\mathbf{R}$ and $\mathbf{G}$ in the cost functional (6). Figure 6 shows some results for the application of ME uncertainty and the use of actuator 1/sensor 1 for control. A maximum error of 5% ($b_0 = 0.05$) for each identified modal frequency and each modal damping ratio was assumed, which leads to twelve uncertainty inputs/outputs. Figure 6 a) shows some results for a model error of -5% and Figure 6 b) the results for a model error of +5%. The damping is good for the first six

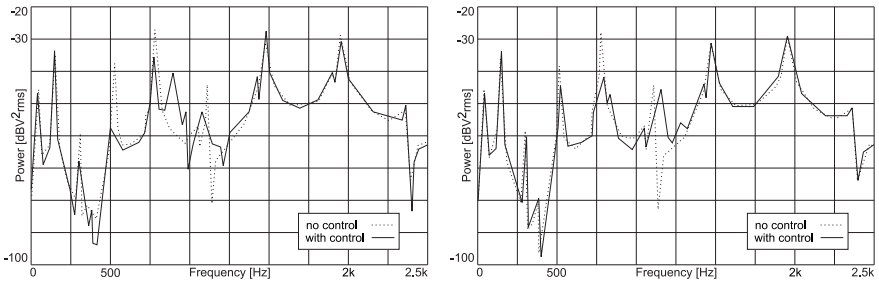

Fig. 5: Power spectrum of the voltage at ceramic 2; NHFD uncertainty.
a) Actuator 4, sensor 1, **b)** Actuator 1, collocated sensor

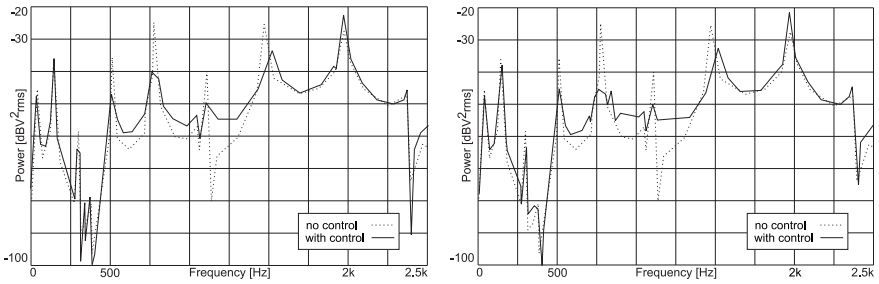

Fig. 6: Power spectrum of the voltage at ceramic 2; ME uncertainty, Actuator 1, collocated sensor.
a) Model error -5%, **b)** Model error +5%

modes, but some spillover occurs in the higher frequency range. Again the achievable suppression depends heavily on the matrices $\mathbf{R}$ and $\mathbf{G}$ in the cost functional (6).

8 Summary

A robust LQG control which is robust against spillover or parameter uncertainties has been successfully applied for the vibration control of a beam. The control design has been demonstrated theoretically, and the implementation of the specific uncertainties against spillover and parameter errors have been shown. The model, which was used for the controller design has been obtained with the help of piezoelectric patches bonded onto the structure. Depending on the identified modal characteristics of the structure different patches have been found to be best suited as actuators and sensors.
Future work will concentrate on the simultaneous application of the NHFD and ME uncertainties in order to achieve a robust control for both uncertainties and the comparison with other control concepts.

References

[1] Balmés, Etienne: *Structural Dynamics Toolbox for Matlab*. Scientific Software, 1998

[2] Dimitriadis, E.K.; Fuller, C.A.; Rogers, C.A.: *Piezoelectric actuators for distributed vibration excitation of thin plates*. **In:** Journal of Vibration and Acoustics 113 (1991), pp. 100 – 107

[3] Falangas, Eric T.; Dworak, J.A.; Koshigoe, Shozo: *Controlling Plate Vibrations Using Piezoelectric Actuators*. **In:** IEEE Control Systems (1994), pp. 34–41

[4] Kim, S.J.; Jones, J.D.: *Optimal Design of Piezoactuators for Active Noise and Vibration Control*. **In:** AIAA Journal 29 (1991), December, Nr. 12, pp. 2047 – 2053

[5] Kuhnen, K.; Janocha, H.: *An Operator-Based Controller Concept for Smart Piezoelectric Actuators*. IUTAM-Symposium Smart Structures and Structronic Systems. Magdeburg, Germany, 26.-29. September 2000

[6] Lim, Young-Hun; Varadan, Vasundara V.; Varadan, Vijay K.: *Closed–Loop Finite–Element Modeling of Active Structural Damping in the Frequency Domain*. **In:** Smart Materials and Structures 6 (1997), pp. 161 – 168

[7] Preumont, André: *Active Structures for Vibration Suppressions and Precision Pointing*. **In:** Journal of Structural Control 2 (1995), June, Nr. 1, pp. 49–63

[8] Petersen, Ian R.; Ugrinovskii, Valery A.; Savkin, Andrey V.: *Robust Control Design Using H_∞ Methods*. Springer-Verlag London Berlin Heidelberg, 2000

[9] Schwinn, A.; Janocha, H.: *Self-Configurable Actuator-Sensor Array for Active Vibration Suppression*. Materialsweek 2000. Munich, Germany, September 2000

[10] Welch, P.D.: *The Use of Fast Fourier Transform for the Estimation of Power Spectra: A Method Based on Time Averaging Over Short, Modified Periodograms*. **In:** IEEE Trans. Audio Electroacoust. AU-15 (1967), June, pp. 70–73